

M2a Macrophage-Dominant Microenvironment in Inflammation Attenuation and Wound Healing of Human Corneal Endothelial Cells

Seung Hyeun Lee,^{1,3} Ahra Koh,^{1,3} Soo Jin Lee,¹ Hun Lee,⁴ and Kyoung Woo Kim^{1,5}

¹Chung-Ang Ocular Surface Restoration via Immune-Inflammation Alleviation (CORIA) Laboratory, Seoul, Republic of Korea

²Department of Ophthalmology, Chung-Ang University Gwangmyeong Hospital, Gwangmyeong-si, Gyeonggi-do, Republic of Korea

³Chung-Ang University Graduate School, Seoul, Republic of Korea

⁴Department of Ophthalmology, Asan Medical Center, University of Ulsan College of Medicine, Seoul, Republic of Korea

⁵Department of Ophthalmology, Chung-Ang University College of Medicine, Chung-Ang University Hospital, Seoul, Republic of Korea

Correspondence: Kyoung Woo Kim, Department of Ophthalmology, Chung-Ang University College of Medicine, Chung-Ang University Hospital, 102 Heukseok-ro, Dongjak-gu, Seoul 06973, Republic of Korea; kkanssa@cau.ac.kr.

Received: November 22, 2024

Accepted: May 17, 2025

Published: June 10, 2025

Citation: Lee SH, Koh A, Lee SJ, Lee H, Kim KW. M2a macrophage-dominant microenvironment in inflammation attenuation and wound healing of human corneal endothelial cells. *Invest Ophthalmol Vis Sci*. 2025;66(6):35. <https://doi.org/10.1167/iovs.66.6.35>

PURPOSE. To investigate the anti-inflammatory and wound-healing effects of an M2a macrophage-dominant microenvironment on human corneal endothelial cells (HCECs) in vitro.

METHODS. Two in vitro corneal endothelial inflammation models were developed: a lipopolysaccharide (LPS)-induced inflammation-only model and a dual inflammation-and-wound model. HCECs were co-cultured with M2a macrophages or treated with M1 macrophage-derived exosomes (M1-exo), M2a macrophage-derived exosomes (M2a-exo), or epidermal growth factor (EGF)-preconditioned M2a-derived exosomes (EGF-M2a-exo). Gene and protein expression of inflammatory markers was assessed, and HCEC proliferation was evaluated using cell growth curves.

RESULTS. Scratch wounding alone did not induce significant inflammation in HCECs, whereas LPS stimulation combined with scratch wounding markedly increased inflammatory responses. In the inflammation-only model, co-culture with M2a macrophages or M2a-exo treatment significantly suppressed LPS-induced upregulation of *IL6*, *IL1B*, and *ICAM1* at the mRNA level in HCECs and reduced IL-6 protein secretion. In the dual inflammation-and-wound model, M2a-exo showed limited efficacy, but EGF-M2a-exo significantly reduced inflammatory marker expression. Cell growth analysis revealed that M2a-exo treatment promoted faster HCEC proliferation compared to M1-exo treatment under non-inflammatory conditions, despite no significant differences in cell cycle-related genes. In LPS-stimulated HCECs, EGF-M2a-exo treatment restored proliferation to levels comparable with non-inflammatory controls by day 5.

CONCLUSIONS. An M2a macrophage-dominant microenvironment demonstrates anti-inflammatory and regenerative effects on inflamed HCECs. EGF preconditioning enhances these properties, suggesting a potential therapeutic approach for managing corneal endothelial inflammation and injury.

Keywords: corneal endothelium, exosome, inflammation, M2a macrophage, wound healing

The corneal endothelium plays a critical role in maintaining corneal transparency and visual acuity by regulating corneal hydration through its barrier and pump functions.¹ Unlike many other cell types, human corneal endothelial cells (HCECs) have limited proliferative capacity in vivo.² Consequently, when the corneal endothelium is damaged by injury or disease, the healing process relies primarily on cell enlargement and migration rather than proliferation.³ Excessive inflammation during corneal endothelial wound healing can lead to further cell loss, compromised barrier function, and corneal edema.^{4,5} If left uncontrolled, this can result in bullous keratopathy and vision loss and may necessitate

corneal transplantation.⁶ Therefore, modulating inflammation to support regenerative healing of the corneal endothelium holds significant clinical value.

Macrophages play critical roles in corneal homeostasis, inflammation, and wound healing.⁷ Recent studies have shown that macrophages populate the corneal stroma, including regions near the corneal endothelium.^{8,9} These corneal macrophages express typical markers such as F4/80, CD11b, and CD68, constituting approximately 50% of all immune cells in the cornea.¹⁰ Macrophages can be broadly classified into distinct functional subtypes, with M1 and M2 macrophages being the most well-characterized. M1

macrophages are generally considered pro-inflammatory and are involved in host defense against pathogens, whereas M2 macrophages are associated with tissue repair, wound healing, and resolution of inflammation.^{11,12} The balance between these subtypes is critical for maintaining corneal homeostasis and orchestrating appropriate responses to injury or infection.¹³

M2 macrophages can be further subdivided into M2a, M2b, and M2c subtypes based on their activating stimuli and functional characteristics.¹⁴ M2a macrophages, induced by interleukin (IL)-4 or IL-13, are associated with wound healing and tissue repair functions.¹⁵ They also secrete anti-inflammatory mediators, such as IL-10 and transforming growth factor beta (TGF- β), along with growth factors that promote angiogenesis and extracellular matrix remodeling.¹⁶ Interactions between macrophages and corneal endothelial cells have been observed in various contexts. For example, macrophages have been implicated in mediating corneal endothelial rejection following transplantation.¹⁷ Additionally, macrophages can accumulate on the corneal endothelium in response to inflammatory stimuli, forming multinucleated giant cells.^{18,19} However, the specific effects of M2a macrophages on corneal endothelial wound healing and inflammation remain poorly understood.

Exosomes are small extracellular vesicles (30–150 nm) that play important roles in intercellular communication by transferring proteins, lipids, and nucleic acids.²⁰ In our previous study, M1 macrophage-derived exosomes (M1-exo) were shown to induce inflammatory and vasculogenic signals in HCECs.²¹ Recent studies have demonstrated that macrophage-derived exosomes can modulate inflammation and tissue repair in various disease models.^{22,23} However, the potential therapeutic effects of M2a macrophage-derived exosomes on corneal endothelial wound healing have not been investigated.

This study examined the anti-inflammatory and wound healing effects of M2a macrophage-derived exosomes on inflamed corneal endothelial cells *in vitro*. We hypothesized that these exosomes could attenuate inflammatory responses and promote regenerative healing in a model of corneal endothelial inflammation and injury. Additionally, we investigated whether the anti-inflammatory properties of epidermal growth factor (EGF) could further enhance the therapeutic potential of M2a-derived exosomes, as suggested by previous findings on the modulatory effects of EGF on M1 macrophage-derived exosomes.²¹

METHODS

Study Approval

Study approval was obtained from the Institutional Review Boards at Chung-Ang University Hospital (IRB Approval No. 2106-006-465) for the usage of cadaveric eye tissues in corneal endothelial cell culture, following the tenets of the Declaration of Helsinki.

Isolation and Culture of HCECs

The HCECs used in this study were isolated from the peripheral rims of donor corneas following penetrating keratoplasty procedures. All donors were Asian and included four individuals (56-year-old male, 63-year-old male, 57-year-old female, and 61-year-old female), each with an endothelial cell density exceeding 2400 cells/mm².

The comprehensive protocol was developed based on our previously established methodology.^{21,24} Human corneal tissues, free from prior eye diseases, were obtained for the purpose of corneal transplantation and stored at 4°C in storage medium (Optisol-GS; Bausch & Lomb, Bridgewater, NJ, USA). After excising the central 8-mm round section of the cornea for transplantation, the corneal tissues at the periphery were used for the culture of HCECs. Corneal tissue was washed six times with phosphate-buffered saline (PBS; Welgene Biotech, Gyeongsan-si, Korea) containing an antibiotic solution of penicillin and streptomycin. For the isolation of HCECs, Descemet's membrane–corneal endothelia were carefully stripped off and digested with 1-mg/mL collagenase A (#07434; STEMCELL Technologies, Vancouver, BC, Canada) at 37°C for 2 hours. The HCECs were detached from Descemet's membrane and placed in medium (Gibco Opti-MEM-I, #31985070; Thermo Fisher Scientific, Waltham, MA, USA) for corneal endothelial cell growth, supplemented with 8% fetal bovine serum (FBS), 0.08% chondroitin sulfate, 20 μ g/mL of ascorbic acid, 200 μ g/mL of CaCl₂, 10 μ L/mL of multivitamin solution, 100 μ g/mL of pituitary extract, 5 ng/mL of EGF, 20 ng/mL of nerve growth factor, 50 ng/mL of gentamicin, and 100 units/mL penicillin/ streptomycin. HCECs were washed and collected after centrifugation at 1200 rpm for 5 minutes. They were then plated onto tissue culture dishes coated with a mixture of bovine serum albumin (BSA), collagen type IV, and fibronectin, to facilitate attachment. The cells were incubated at 37°C in a humidified incubator with 5% CO₂. When the cells reached 80% to ~90% confluency, they were subcultured using Gibco TrypLE Express Enzyme (#12604; Thermo Fisher Scientific). Experiments were performed using cells at the third passage.

In Vitro Corneal Endothelial Inflammation-Only Modeling and Dual Inflammation-and-Wound Modeling Using HCECs

HCECs were seeded in six-well plates at a density of 1.5×10^5 cells per well and were cultured for 48 hours to achieve a confluent monolayer (>90% confluency). To create the *in vitro* corneal endothelial inflammation-only model, LPS (1 μ g/mL) was applied to HCECs for 24 hours to induce inflammation. For the *in vitro* corneal endothelial dual inflammation-and-wound model, HCECs were cultured for 48 hours and a straight wound was created in the monolayer by scraping with a 200- μ L pipette tip (yellow tip), as previously described.²⁴ LPS (1 μ g/mL) was then applied to HCECs for 24 hours following the scratch procedure. The concentration of 1 μ g/mL LPS was selected based on preliminary dose–response experiments (0.1, 0.5, and 1 μ g/mL), which showed a significant induction of IL-6 and IL-1B expression at this concentration (see Supplementary Fig. S1).

M1 and M2a Macrophage Polarization

We induced M1 or M2a macrophages from the THP-1 cell line (TIB-202; American Type Culture Collection, Manassas, VA, USA) following well pre-established protocols.^{21,25–27} THP-1 cells were cultured in the RPMI 1640 medium (Welgene Biotech, Gyeongsan-si, Korea) with the appropriate supplements. After the cells were seeded in six-well plates, they were differentiated into

M0 macrophages using 50-nM phorbol 12-myristate 13-acetate (PMA, #P8139; Sigma-Aldrich, St. Louis, MO, USA) for 24 hours. Lipopolysaccharide (LPS, O111:B4, #L2630, 100 ng/mL; Sigma-Aldrich) and recombinant human interferon-gamma (IFN- γ , #570216, 20 ng/mL; BioLegend, San Diego, CA, USA) were treated for 24 hours for M1 macrophage polarization. Recombinant human IL-4 (#574004, 20 ng/mL; BioLegend) and recombinant human IL-13 (#571104, 20 ng/mL; BioLegend) were treated for 24 hours for M2a macrophage polarization.

Co-Culture of M2a Macrophages and HCECs

HCECs were seeded in six-well plates at a density of 1.5×10^5 cells/well and cultured for 48 hours. Following the induction of inflammation and scratching in HCECs to prepare for the two types of in vitro corneal endothelial inflammation models, the inflammatory HCECs were co-cultured with M2a macrophages for 48 hours. Co-cultures were performed using a Transwell insert with a pore size of 0.4 μ m (SPL Life Sciences, Pocheon-si, South Korea), which were placed into the six-well plates. M2a macrophages were resuspended in RPMI 1640 medium at a density of 1×10^5 cells per insert. The co-cultures of M2a macrophages and HCECs were incubated undisturbed at 37°C in a humidified 5% CO₂ incubator for 48 hours. RNA was subsequently extracted from HCECs (in the six-well plates) for further analysis.

Extraction of Exosomes From Macrophages

M1 and M2a macrophages were incubated in media containing exosome-depleted FBS (#EXO-FBS-250A-1; System Biosciences, Palo Alto, CA, USA). M2a macrophages were treated with recombinant human EGF (#E9644, 10 ng/mL; Sigma-Aldrich) for 24 hours for EGF preconditioning. The supernatant was collected for exosome isolation. ExoQuick-TC (#EXOTC50A-1; System Biosciences) was used to precipitate exosomes from the culture medium of M1 or M2a macrophages. Briefly, the medium was centrifuged at 2500 rpm for 10 minutes to remove cells and debris. The supernatant was collected and filtered using a 0.22- μ m pore filter (#SLGVR33RS; Merck Millipore, Rahway, NJ, USA). The medium was then mixed with ExoQuick-TC and incubated overnight at 4°C. Finally, exosomes were centrifuged at 13,000 rpm for 1 hour at 4°C, and the pellets were resuspended in PBS and stored at -80°C. The protein content of the exosomes was measured using a Pierce BCA Protein Assay Kit (#23227; Thermo Fisher Scientific). The size distribution and concentration of purified exosomes were analyzed using nanoparticle tracking analysis with the Malvern NanoSight NS300 (Malvern Panalytical, Malvern, Worcestershire, UK) and the NanoSight NTA 3.4 Analytical, as described in our previous study.²¹

Exosome Staining and Tracking

The labeling of exosomes with dye was performed as previously established.^{21,25} For exosome labeling, we used the PKH26 Red Fluorescent Cell Linker Dye (#PKH26GL; Sigma-Aldrich) in accordance with the manufacturer's instructions. Exosomes were stained by mixing 1 μ L of PKH26 dye with 200 μ L of Diluent C from the kit and incubating the solution at room temperature for 5 minutes. To stop the labeling process, an equal volume of 10% BSA was

added, followed by repurification of the exosomes using a method of total exosome isolation reagent precipitation. The culture medium of HCECs was replaced with a medium containing PKH26-labeled exosomes derived from M1 or M2a macrophages. The cells were incubated with exosomes for 24 hours and then fixed with 4% paraformaldehyde after being washed with Gibco Dulbecco's Phosphate-Buffered Saline (DPBS; Thermo Fisher Scientific). Cells were mounted using VECTASHIELD Antifade Mounting Medium with DAPI (#H-1200-10; Vector Laboratories, Newark, CA, USA) and were analyzed using an inverted fluorescence microscope (DMi8; Leica, Wetzlar, Germany).

Exosome Treatment

For exosome treatment, M1 macrophage-, M2a macrophage-, or EGF-preconditioned M2a macrophage-derived exosomes (10 μ g/mL) were applied to HCECs with LPS simultaneously for 24 hours to create the in vitro inflammation-only model and the dual inflammation-and-wound model. Cell culture plates were maintained at 37°C in a humidified 5% CO₂ incubator. The concentration of 10 μ g/mL was selected based on a preliminary dose-response experiment (5, 10, and 20 μ g/mL) (see Supplementary Fig. S2), which demonstrated that this dose exerts significant anti-inflammatory effects on *IL6*, *IL1B*, and *ICAM1* expression in HCECs.

Cell Growth Assay

HCECs were seeded into 96-well plates at a density of 1×10^4 cells/well for 24 hours. HCECs were treated with LPS and M1 macrophage-, M2a macrophage-, or EGF-preconditioned M2a macrophage-derived exosomes (10 μ g/mL). Cell proliferation was measured after 0, 1, 2, 3, 4, and 5 days of culture. Then, 10 μ L of Cell Counting Kit-8 (CCK-8) reagent (#ALX-850-039-KI01; Enzo Life Sciences, Farmingdale, NY, USA) was added into each well, and the culture plates were incubated in 5% CO₂ at 37°C for 2 hours. Subsequently, 100 μ L of each culture solution was transferred to a separate 96-well plate, and the optical density (OD) at 450 nm was measured using a SpectraMax i3x Multi-Mode Microplate Reader (Molecular Devices, San Jose, CA, USA). The OD values obtained from the experiment were plotted against the calibration curve to quantify the cell count.

Purification of Total RNA and Real-Time Quantitative Reverse Transcription Polymerase Chain Reaction

Total RNA was extracted from the cells using NucleoZOL (#740404.200; Macherey-Nagel, Düren, Germany) following the manufacturer's protocol. Single-stranded complementary DNA (cDNA) was synthesized from the total RNA (1 μ g) using the RevertAid First Strand cDNA Synthesis Kit (#K1622; Thermo Fisher Scientific). Real-time quantitative reverse transcription polymerase chain reaction (qRT-PCR) was performed using a QuantStudio 3 Real-Time PCR System (Applied Biosystems, Foster City, CA, USA). Relative gene expression levels were calculated using the $2^{-\Delta\Delta Ct}$ method, with normalization to the reference gene 18S ribosomal RNA. Sequences of PCR primers are shown in the Table.

TABLE. Sequences of PCR Primers

Gene		Primer Sequence	Product Size (bp)	Accession No.
IL1B	Sense	CCACAGACCTTCCAGGAGAATG	131	NM_000576.3
	Antisense	GTGCAGTTCAGTGATCGTACAGG		
IL6	Sense	AATAACCACCCCTGACCCAAC	168	NM_000600.4
	Antisense	AATCTGAGGTGCCCATGCTAC		
MRC1	Sense	CATCAGGGTGCAAGGAAGGT	202	NM_002438.4
	Antisense	GTCCAGGCACTGAAAGTGGA		
TJP1	Sense	GAACGAGGCATCATCCCTAA	218	NM_001330239.1
	Antisense	CCAGCTTCTCGAAGAACCAC		
ICAM1	Sense	AGGATGGCACTTTCCCACTG	131	NM_000201.3
	Antisense	GGAGAGCACATTACGGTCA		
PTEN	Sense	TCCCAGACATGACAGCCATC	189	NM_000314.6
	Antisense	GCTTTGAATCCAAAAACCTTACTAC		
CDC25A	Sense	ACCTCAGAAGCTGTTGGGATG	174	NM_001789.2
	Antisense	TGGAGTCCATGAGAGTGCAG		
18S rRNA	Sense	CGGCGACGACCCATTGGAAC	60	NR_145820.1
	Antisense	GAATCGAACCCTGATTCCCCGTC		

Enzyme-Linked Immunosorbent Assay

Concentrations of IL-1 β and IL-6 in the supernatants of HCECs co-cultured with M2a macrophages or treated with exosomes were measured using a human IL-1 β ELISA Kit (#BMS224-2; Thermo Fisher Scientific) and a human IL-6 ELISA Kit (#EH2IL6; Thermo Fisher Scientific), according to the manufacturer's instructions. Briefly, the culture supernatants were collected and centrifuged at 13,000 rpm for 30 minutes at 4°C. Then, 100 μ L of the clarified supernatant was used to measure the levels of IL-1 β and IL-6. The concentrations were calculated based on a standard curve, generated from absorbance values measured at 450 nm using the SpectraMax i3x Multi-Mode Microplate Reader.

Statistical Analysis

Given the technical challenges of culturing HCECs and the limited availability of donor tissue, HCECs were harvested from four independent human donors, and each sub-experiment was conducted using cells derived from a distinct single representative donor. Although this approach does not account for inter-donor variability within individual experiments, it reflects a widely used and contextually appropriate strategy for in vitro studies involving rare or difficult-to-culture primary human cells. Our objective was to model the effects of inflammatory stimuli and therapeutic interventions, rather than to evaluate donor-dependent differences.

Prism 10 (GraphPad Software, Boston, MA, USA) was used for the statistical analysis. When the data were compared among three or more groups, data were analyzed using ANOVA followed by Tuckey's post hoc test. In addition, to compare data between two groups, Student's *t*-test was used. Data within graphs are presented as the mean \pm standard error. Differences were considered statistically significant for *P* < 0.05.

RESULTS

Development of Two In Vitro Corneal Endothelial Inflammatory Models

The corneal endothelium may be damaged either by inflammatory insults alone, such as in uveitis and allogeneic rejection,

or by mechanical injury accompanied by inflammation, as observed in intraocular surgeries and trauma.^{28–30} To model these conditions, we developed two types of in vitro inflammatory models using HCECs: an LPS-induced inflammation-only model and a dual inflammation-and-wound model incorporating scratch injury (Figs. 1A–C).

LPS stimulation induced significant upregulation of *IL6*, *IL1B*, and *ICAM1* mRNA expression in HCECs, indicating a robust inflammatory response. Among these, the expression of *IL6* and *IL1B* was further enhanced in the dual inflammation-and-wound model (Figs. 1D–F). Consistent with the transcriptional data, ELISA revealed increased IL-6 protein levels in both models, with the highest levels observed in the dual model. In contrast, IL-1 β protein did not significantly increase, despite elevated mRNA expression (Figs. 1G, 1H). Notably, scratch wounding alone without LPS did not induce upregulation of IL-6 or IL-1 β at either the gene or protein level.

Modulation of LPS-Induced Corneal Endothelial Inflammation Through Co-Culture With M2a-Dominant Macrophages

We next evaluated the modulatory effects of M2a-dominant macrophages on LPS-induced inflammation in HCECs in both in vitro models. M2a polarization was confirmed by elevated expression of the M2a marker *MRC1* (CD206) (Supplementary Fig. S3). In the inflammation-only model, co-culture with M2a macrophages significantly reduced the mRNA expression of *IL6* and *IL1B*, whereas *ICAM1* levels remained unchanged (Figs. 2A–D). Consistently, ELISA showed decreased IL-6 protein levels, whereas IL-1 β levels remained unchanged following LPS stimulation or M2a macrophage co-culture (Figs. 2E, 2F). In the dual inflammation-and-wound model, M2a macrophage co-culture also suppressed *IL6* and *IL1B* mRNA expression (Figs. 2G–J), accompanied by a decrease in IL-6 protein secretion (Fig. 2K). However, IL-1 β protein levels remained unaffected (Fig. 2L), consistent with the findings in the inflammation-only condition. Together, these results highlight the anti-inflammatory role of M2a-dominant macrophages, particularly through the attenuation of IL-6-mediated responses, in both the inflammation-only and dual inflammation-and-wound models.

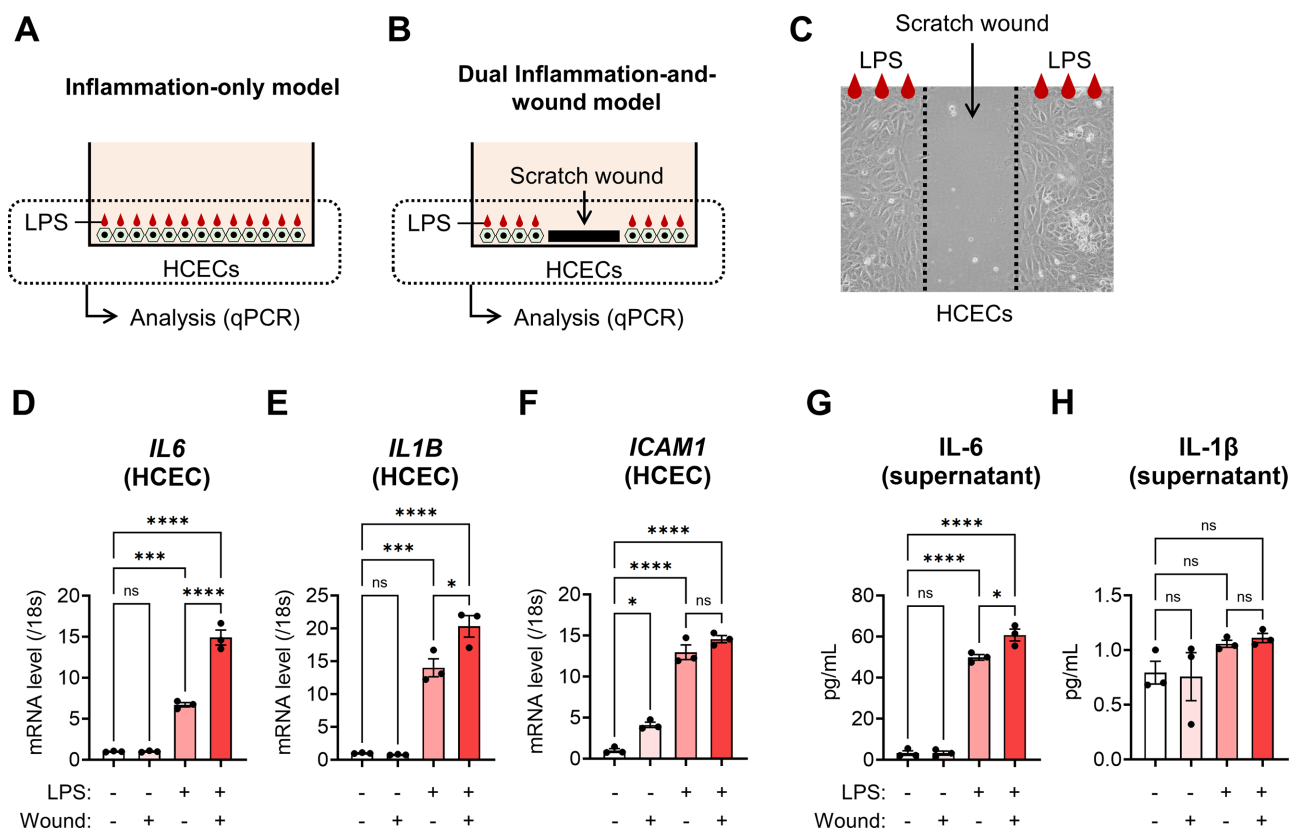


FIGURE 1. In vitro models of human corneal endothelial inflammation and combined inflammation and wound injury, with condition-specific expression of inflammatory markers. (A, B) Schematic diagrams of the inflammation-only model and the dual inflammation-and-wound model using HCECs. (C) Representative image of LPS-stimulated HCECs following mechanical scratch wounding. (D–F) qRT-PCR analysis of *IL6*, *IL1B*, and *ICAM1* mRNA expression in naïve HCECs, wounded-only HCECs, inflammation-only HCECs, and dual inflammation-and-wound model HCECs. (G, H) ELISA analysis of IL-6 and IL-1 β protein levels in the culture supernatants from the corresponding conditions. Data are presented as mean \pm SEM from three samples ($n = 3$). **** $P < 0.0001$, *** $P < 0.001$, * $P < 0.05$; ns, not significant.

Comparative Analysis of Inflammatory Modulation by M1- and M2a-Derived Exosomes in HCECs

Following our findings using a co-culture system (Fig. 2), we further validated the anti-inflammatory effects of macrophage-derived factors by utilizing exosomes, which easily penetrate cells in general,²⁰ including HCECs.²¹ In our previous study, exosomes from M1 macrophages were shown to induce innate immune-related inflammation in cultured HCECs and in murine corneal tissue.²¹ Based on the inflammatory modulatory potential of macrophage-derived exosomes in ocular cells, we isolated exosomes from both M1-dominant (M1-exo) and M2a-dominant (M2a-exo) macrophage populations, and we treated HCECs with each to assess their respective effects on inflammatory marker expression.

Successful uptake of the exosomes by HCECs was confirmed by fluorescent labeling (Fig. 3A). Neither M1-exo nor M2a-exo treatment altered the expression of *TJP1*, which encodes zonular occludens-1, a key tight junction protein in corneal endothelial cells (Fig. 3B). However, M1-exo treatment significantly upregulated the expression of *IL6*, *IL1B*, and *ICAM1*, whereas M2a-exo treatment did not alter the expression levels of these genes compared to untreated controls (Figs. 3C–E). Consistent with the transcriptional data, ELISA results showed a marked increase in IL-6 and

IL-1 β protein levels following M1-exo treatment. In contrast, M2a-exo treatment did not affect protein levels of either cytokine (Figs. 3F, 3G).

Anti-Inflammatory Role of M2a-Derived Exosomes in Corneal Endothelial Inflammatory Models

Given the distinct non-inflammatory profile of M2a-exo compared to M1-exo in HCECs, we next evaluated the anti-inflammatory efficacy of M2a-exo in both the inflammation-only and dual inflammation-and-wound models. In the inflammation-only model, M2a-exo treatment significantly suppressed the LPS-induced upregulation of *IL6*, *IL1B*, and *ICAM1* at the mRNA level (Figs. 4A–D). This suppression was mirrored at the protein level by reduced IL-6 secretion, whereas IL-1 β protein levels remained unchanged (Figs. 4E, 4F). These findings confirm the anti-inflammatory effect of M2a-exo in this model.

EGF has been shown to suppress macrophage inflammation by downregulating pro-inflammatory genes such as *IL6* and *IL1B*.²¹ Exosomes derived from EGF-preconditioned M1 macrophages (EGF-M1-exo) have previously demonstrated anti-inflammatory activity in HCECs and murine corneas.^{21,26} Additionally, in murine corneas, EGF-M1-exo eye drops increased the M2 macrophage marker *ARG1* and mitigated inflammation, demonstrating therapeutic potential.²¹ Based

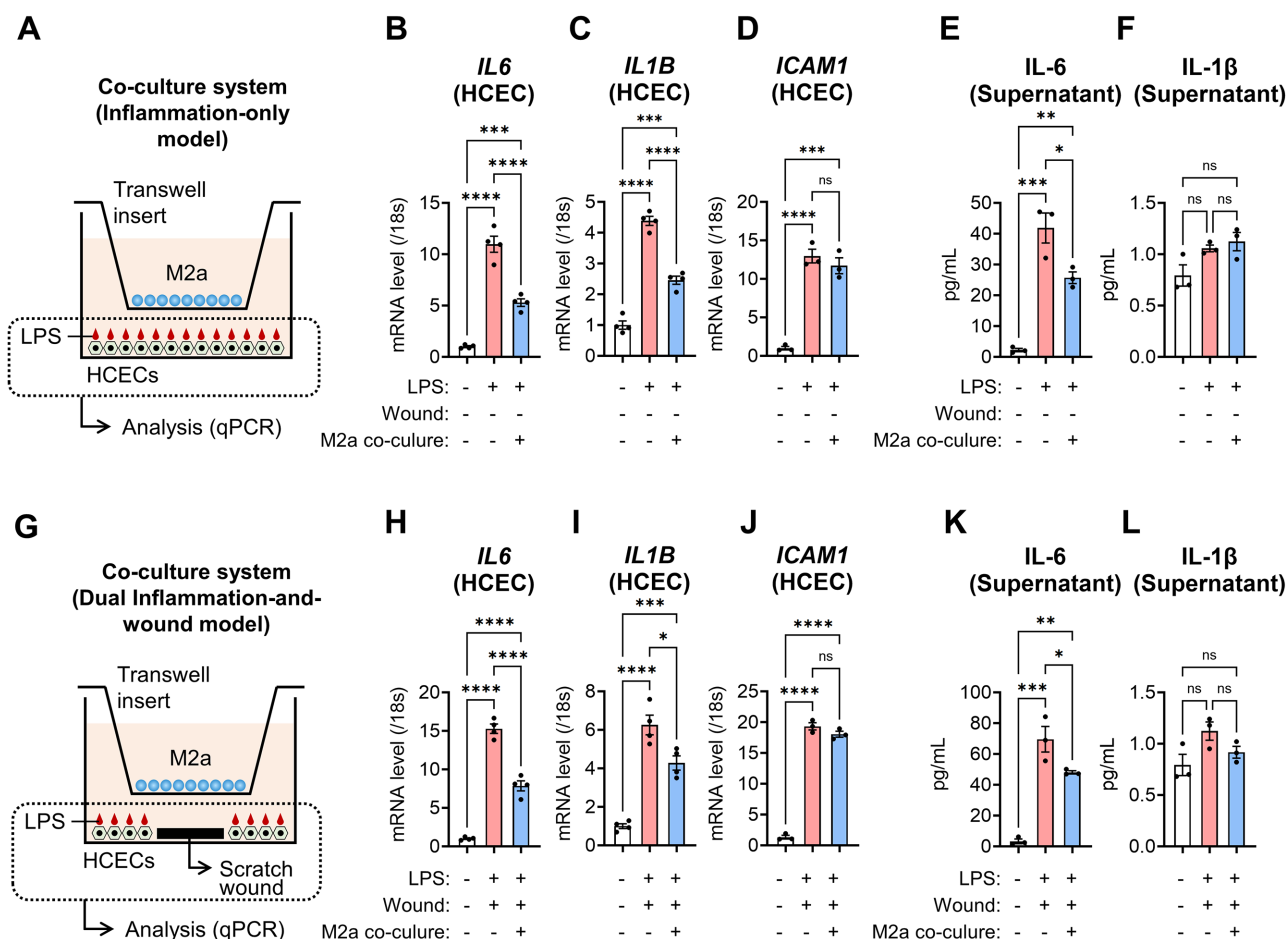


FIGURE 2. Effect of M2a-dominant macrophage co-culture on inflammation in HCECs under two in vitro inflammation models. (A) Schematic diagram of the LPS-induced inflammation-only model using HCECs. (B–D) qRT-PCR analysis of *IL6*, *IL1B*, and *ICAM1* mRNA expression in HCECs with or without M2a-dominant macrophage co-culture in the inflammation-only model. (E, F) ELISA analysis of IL-6 and IL-1β protein levels in the culture supernatants from the same model. (G) Schematic diagram of the dual inflammation-and-wound model using HCECs. (H–J) qRT-PCR analysis of *IL6*, *IL1B*, and *ICAM1* mRNA expression in HCECs with or without M2a-dominant macrophage co-culture in the dual model. (K, L) ELISA analysis of IL-6 and IL-1β protein levels in the culture supernatants from the dual model. Data are presented as mean ± SEM from three or four samples ($n = 3$ or 4). **** $P < 0.0001$, *** $P < 0.001$, ** $P < 0.01$, * $P < 0.05$; ns, not significant.

on these observations, we applied EGF to M2a macrophages to enhance the therapeutic potential of their exosomes. To test this, we first evaluated EGF-preconditioned M2a-exosomes (EGF-M2a-exo) under inflammation-only conditions. Similar to standard M2a-exo, EGF-M2a-exo significantly downregulated *IL6*, *IL1B*, and *ICAM1* mRNA expression and further reduced IL-6 protein levels, whereas IL-1β protein remained unchanged (Figs. 4G–L). These results suggest that, although the inflammation-only model is already responsive to M2a-exo, EGF preconditioning preserves its anti-inflammatory activity.

In contrast, M2a-exo failed to reduce the same inflammatory gene expression in the dual inflammation-and-wound model (Figs. 5A–D), and ELISA confirmed no significant changes in IL-6 or IL-1β protein levels (Figs. 5E, 5F). However, upon treatment with EGF-M2a-exo, a significant downregulation of *IL6*, *IL1B*, and *ICAM1* mRNA expression was observed, along with reduced IL-6 protein levels, whereas IL-1β protein again remained unchanged (Figs. 5G–L). These results indicate that EGF preconditioning restores the anti-inflammatory efficacy of M2a macrophage-derived exosomes, even in more complex inflammatory environments.

Regenerative Potential of M2a-Exo Combined With EGF in HCEC Proliferation

HCECs have limited regenerative capacity in vivo, making wound healing and proliferation critical for maintaining corneal transparency.⁵¹ To assess regenerative potential, cell growth analysis serves as a valuable tool for quantifying proliferation rates and evaluating the efficacy of growth factors or therapeutic agents.^{24,32} Given the previously validated anti-inflammatory role of M2a macrophages (Figs. 1–5), we next investigated whether M2a macrophage-derived exosomes could enhance regenerative responses in HCECs using a 5-day cell proliferation assay.

Under non-inflammatory conditions (i.e., without LPS stimulation), M2a-exo treatment resulted in significantly accelerated proliferation compared to M1-exo treatment on days 2, 4, and 5, with no difference observed on day 3 (Fig. 6A). Notably, by day 5, M2a-exo-treated cells also exhibited a higher proliferation rate than the vehicle group. To explore the underlying mechanism, we assessed the expression of inflammatory markers (*IL6*, *IL1B*) and cell cycle-related genes for phosphatase and tensin homolog (*PTEN*) and cell division cycle 25 homolog A (*CDC25A*) over

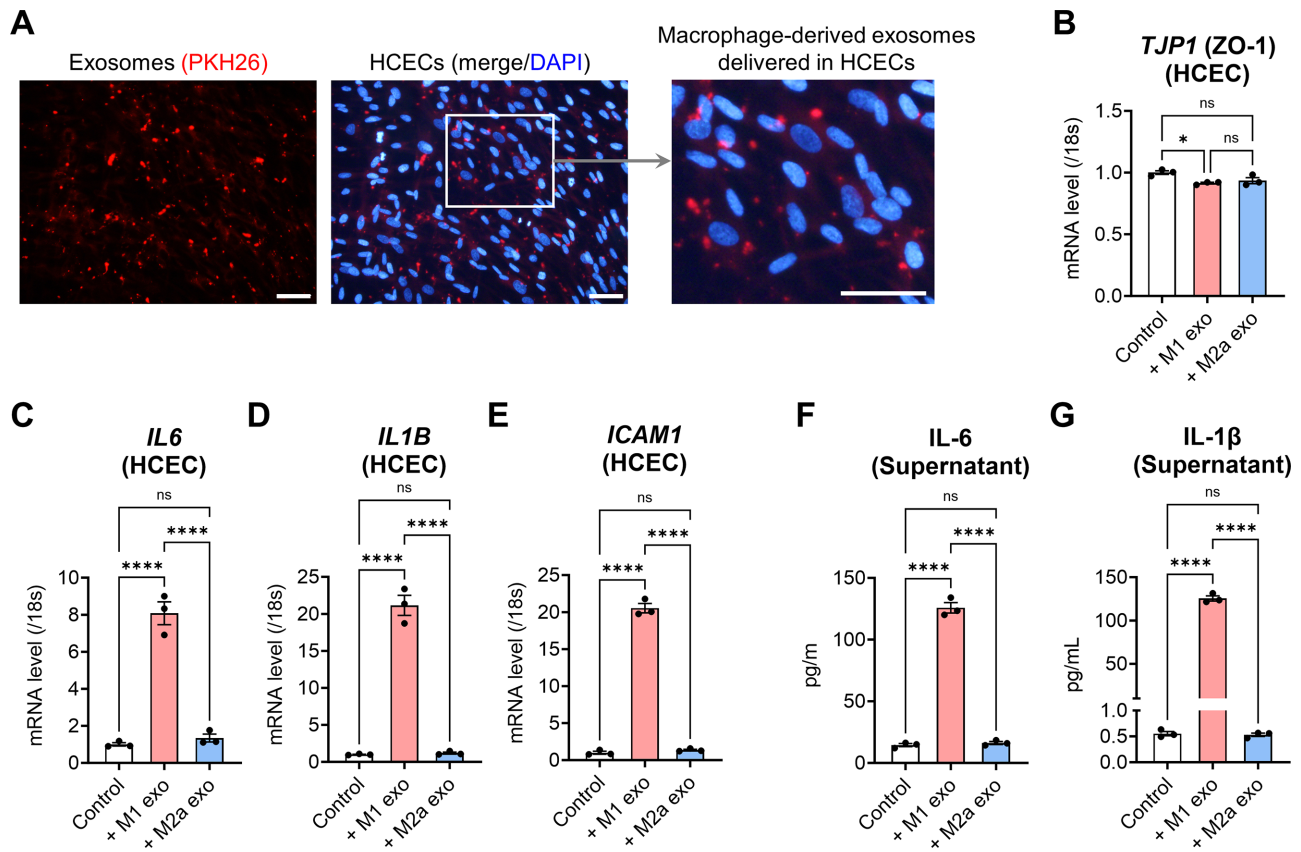


FIGURE 3. Comparison of inflammatory responses induced by M1 and M2a macrophage-derived exosomes in non-inflammatory HCECs. (A) Representative images of PKH26 red dye-labeled macrophage-derived exosomes internalized by cultured HCECs. Scale bars: 100 μ m. (B–E) qRT-PCR analysis of *TJP1*, *IL6*, *IL1B*, and *ICAM1* expression in non-inflammatory HCECs treated with M1-exo or M2a-exo, compared to naïve HCECs. (F, G) ELISA analysis of IL-6 and IL-1 β protein levels in the culture supernatants from the same experimental groups. Data are presented as mean \pm SEM from three samples ($n = 3$). **** $P < 0.0001$, * $P < 0.05$; ns, not significant.

the 5-day period. Although *PTEN* and *CDC25A* expression remained comparable between groups, *IL6* and *IL1B* levels were consistently and significantly lower in M2a-exo-treated cells (Figs. 6B–E), suggesting that the observed proliferative effect is likely driven by inflammation suppression rather than direct activation of the cell cycle.

We then assessed cell proliferation under inflammatory conditions using LPS-stimulated HCECs (Fig. 7). As expected, LPS exposure significantly reduced proliferation from day 2 through day 5 compared to non-inflammatory vehicle controls. Consistent with the limited anti-inflammatory effect observed in the dual inflammation-and-wound model (Figs. 5A–5D), M2a-exo failed to improve proliferation in LPS-stimulated HCECs over the 5-day period. However, EGF-M2a-exo treatment enhanced proliferation on days 4 and 5, with proliferation rates by day 5 being comparable to those of the non-inflammatory vehicle group.

DISCUSSION

The corneal endothelium plays a critical role in maintaining corneal transparency and visual acuity by regulating corneal hydration through its barrier and pump functions.¹ Macrophages, particularly the M2 phenotype, are known to support tissue repair and resolve inflammation in various tissue contexts.^{11,12} Recent studies in particular have emphasized the role of macrophage-derived exosomes

in modulating inflammation and promoting tissue regeneration.^{20–22,26} However, the effects of M2a macrophage-derived exosomes on corneal endothelial inflammation and wound healing remain largely unexplored. In this study, our results demonstrate that both direct co-culture with M2a macrophages and treatment with M2a-derived exosomes reduced inflammatory responses and enhanced healing in in vitro models of corneal endothelial injury. Notably, preconditioning M2a macrophages with EGF further enhanced the anti-inflammatory and regenerative properties of their exosomes in HCECs. These findings underscore the therapeutic potential of M2a macrophage-based interventions for corneal endothelial disorders and highlight the critical role of macrophage phenotype modulation in controlling inflammation and promoting tissue repair.

In this study, we developed two distinct in vitro models to simulate corneal endothelial inflammation: an inflammation-only model and a dual inflammation-and-wound model. These models were subsequently used for all experimental analyses. A wound-only condition was not included, as scratch wounding without LPS stimulation did not induce increased expression of *IL6* or *IL1B* in cultured HCECs. This finding contrasts with previous observations in other cell types, where mechanical injury alone is sufficient to trigger inflammatory signaling. For example, scratch wounding of airway epithelial cells has been shown to upregulate pro-inflammatory cytokines, including IL-6 and IL-1 β .³³ The

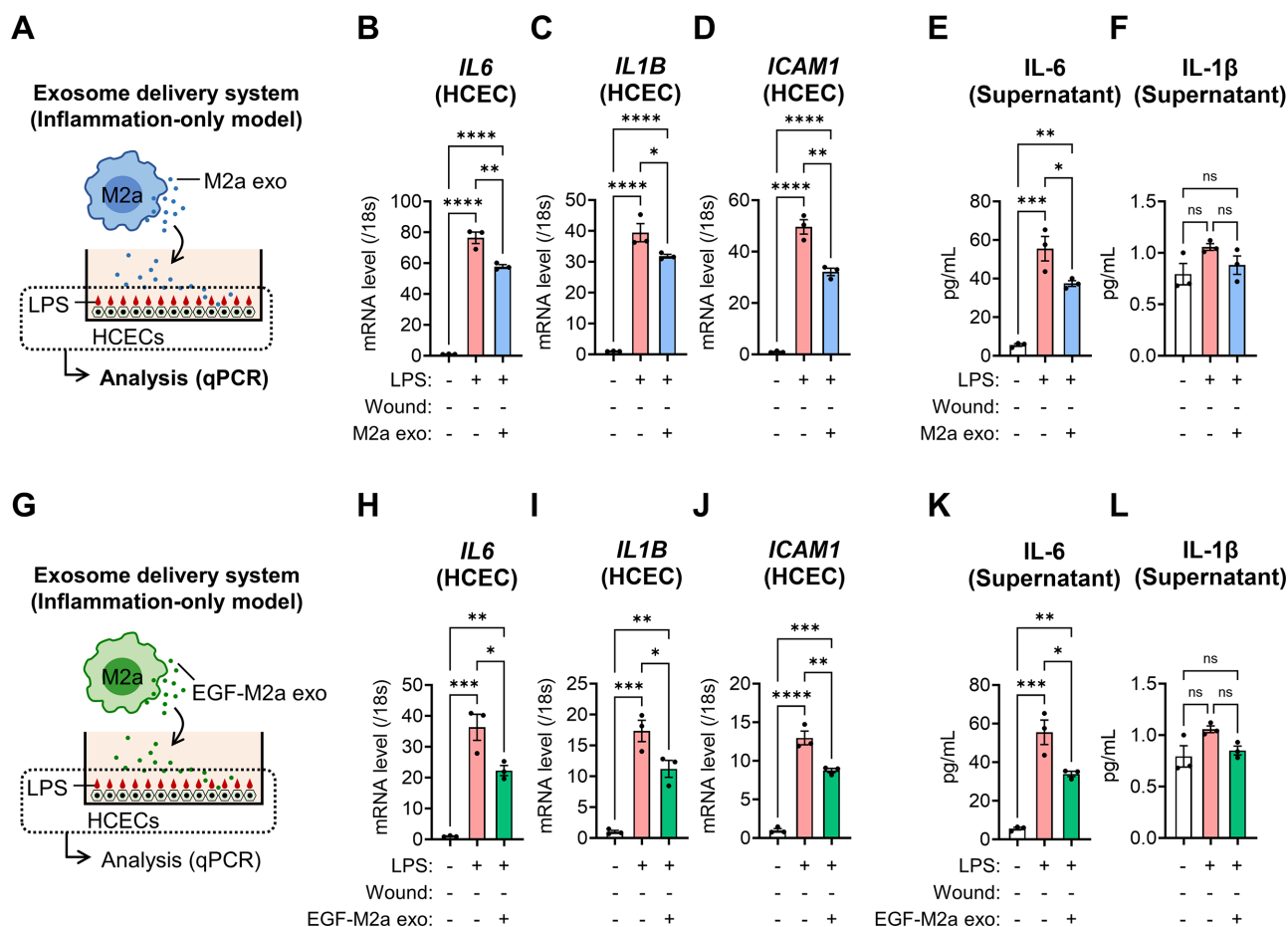


FIGURE 4. Anti-inflammatory effects of M2a-exo and EGF-M2a-exo treatment on inflammatory HCECs in the in vitro corneal endothelial inflammation-only model. **(A)** Schematic illustrations of M2a-exo treatment in LPS-stimulated HCECs (LPS-HCECs) within the inflammation-only model. **(B–D)** qRT-PCR analysis of *IL6*, *IL1B*, and *ICAM1* expression in LPS-HCECs treated with M2a-exo, compared to naïve HCECs. **(E, F)** ELISA analysis of IL-6 and IL-1 β protein levels in the culture supernatants, with or without M2a-exo treatment. **(G)** Schematic illustration of EGF-M2a-exo treatment in the same inflammation-only model. **(H–J)** qRT-PCR analysis of *IL6*, *IL1B*, and *ICAM1* expression in LPS-HCECs treated with EGF-M2a-exo compared to naïve HCECs. **(K, L)** ELISA analysis of IL-6 and IL-1 β protein levels in the culture supernatant, with or without EGF-M2a-exo treatment. Data are presented as mean \pm SEM from three samples ($n = 3$). **** $P < 0.0001$, *** $P < 0.001$, ** $P < 0.01$, * $P < 0.05$; ns, not significant.

lack of a comparable response in HCECs may indicate that these cells possess intrinsic mechanisms to maintain immune quiescence, which is crucial for preserving corneal transparency. Supporting this, previous reports have shown that, even with some degree of endothelial cell loss, phacoemulsification causes only minimal inflammatory changes in the corneal endothelium.³⁴

Interestingly, although *IL6* and *IL1B* mRNA expression levels were significantly elevated in both inflammation models, only IL-6 showed a corresponding increase at the protein level. In contrast, IL-1 β protein was not detected at significantly elevated levels by ELISA, despite its transcriptional upregulation. This discrepancy may reflect a lack of conversion from pro-IL-1 β to its mature, secreted form—a process that requires inflammasome activation and caspase-1-dependent cleavage. Without this maturation step, pro-IL-1 β remains intracellular and is not captured by standard ELISA assays, which typically detect only the active cytokine.³⁵

M2a macrophage-derived exosomes significantly reduced the expression of pro-inflammatory markers, including *IL6*, *IL1B*, and *ICAM1*, in LPS-stimulated HCECs

under inflammation-only conditions, confirming their anti-inflammatory effects. This observation is consistent with previous studies reporting the anti-inflammatory properties of M2 macrophages and their secreted factors.^{22,23,36} Our findings extend this concept to HCECs, underscoring the potential of M2a-exo as a therapeutic strategy for managing corneal endothelial inflammation. Interestingly, M2a-exo alone was not effective in suppressing inflammation in the dual inflammation-and-wound model. This suggests that the anti-inflammatory efficacy of M2a-exo may depend on the specific inflammatory context and the severity or complexity of the insult.

In this study, mechanical wounding was employed as an additional inflammatory stressor rather than as a model to evaluate regenerative outcomes such as wound closure or morphological restoration. Therefore, the assessment of wound healing kinetics or full recovery of HCEC morphology was beyond the scope of this study and remains a key limitation.

Although intercellular adhesion molecule 1 (ICAM-1) is not routinely included in standard inflammatory marker panels and may be less familiar to some readers, we included

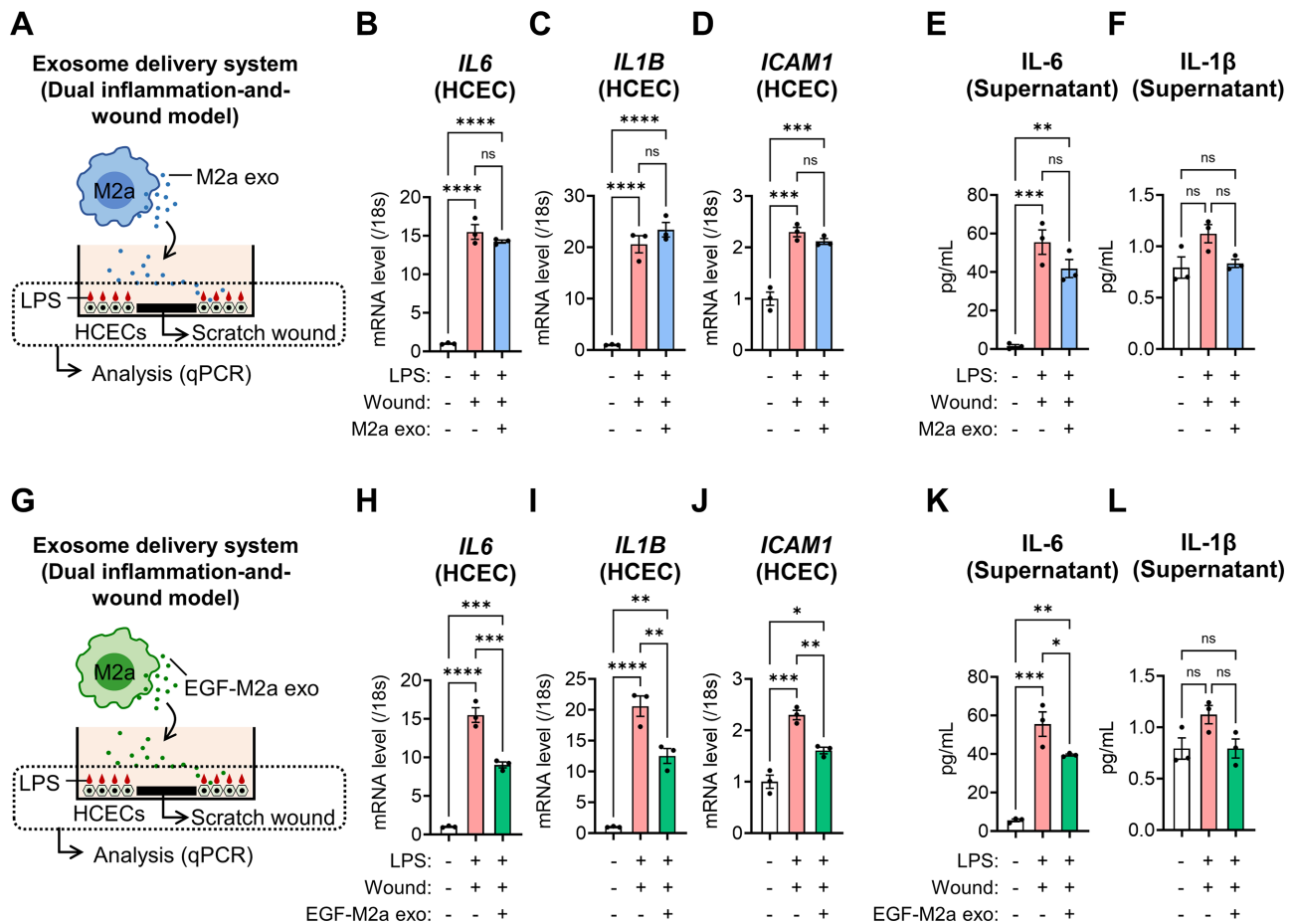


FIGURE 5. Limited anti-inflammatory efficacy of M2a macrophage-derived exosomes and enhanced effects of EGF preconditioning in the in vitro dual inflammation-and-wound model using HCECs. **(A)** Schematic illustrations of M2a-exo treatment in LPS-HCECs within the dual inflammation-and-wound model. **(B–D)** qRT-PCR analysis of *IL6*, *IL1B*, and *ICAM1* mRNA expression in the dual model with or without M2a-exo treatment. **(E, F)** ELISA analysis of IL-6 and IL-1β protein levels in the culture supernatant with or without M2a-exo treatment. **(G)** Schematic illustrations of EGF-M2a-exo treatment in LPS-HCECs in the same dual model. **(H–J)** qRT-PCR analysis of *IL6*, *IL1B*, and *ICAM1* mRNA expression with or without EGF-M2a-exo treatment compared to naïve HCECs. **(K, L)** ELISA analysis of IL-6 and IL-1β protein levels in the culture supernatant with or without EGF-M2a-exo treatment. Data are presented as mean ± SEM from three samples ($n = 3$). **** $P < 0.0001$, *** $P < 0.001$, ** $P < 0.01$, * $P < 0.05$; ns, not significant.

it due to its well-established role in endothelial immunobiology. Although its expression is minimal in quiescent corneal endothelial cells, it is markedly upregulated under inflammatory conditions—particularly in response to IL-1β, tumor necrosis factor alpha, and IFN-γ, as demonstrated by Pavlack et al.³⁷ This cytokine-inducible expression allows ICAM-1 to act as a key immunologic mediator in conditions such as uveitis and corneal graft rejection, by facilitating leukocyte recruitment to the corneal endothelium.

One of the key findings of this study is that EGF-conditioned M2a-exo exhibit enhanced anti-inflammatory activity compared to standard M2a-exo in the dual inflammation-and-wound model. EGF-M2a-exo significantly suppressed the upregulation of *IL6*, *IL1B*, and *ICAM1* in this more complex inflammatory setting. These findings are in line with previous reports showing that EGF modulates macrophage phenotype and function, promoting anti-inflammatory behavior.^{21,26,38} Our data suggest that EGF enhances the immunomodulatory potential of M2a macrophages, resulting in exosomes with superior anti-inflammatory properties.

In addition to their immunomodulatory effects, M2a-exo treatment promoted HCEC proliferation under non-inflammatory conditions, with a corresponding reduction in *IL6* and *IL1B* expression. This implies that their pro-regenerative effects may be mediated, at least in part, through inflammation suppression rather than direct activation of cell cycle-related pathways, as supported by the minimal changes in *PTEN* and *CDC25A* observed in Figure 6. This observation is consistent with the established role of chronic inflammation in impairing tissue regeneration and wound healing.^{39,40} Importantly, EGF-M2a-exo treatment restored proliferation in LPS-stimulated HCECs, achieving levels comparable to non-inflammatory controls by day 5. These findings indicate that EGF-M2a-exo not only suppress inflammation but also promote regeneration in inflamed endothelial cells, reflecting the dual role of EGF in both anti-inflammatory signaling and wound repair.⁴¹

Although our study applied a single exosome concentration based on anti-inflammatory efficacy, it remains unclear whether higher doses of EGF-M2a-exo could directly stimu-

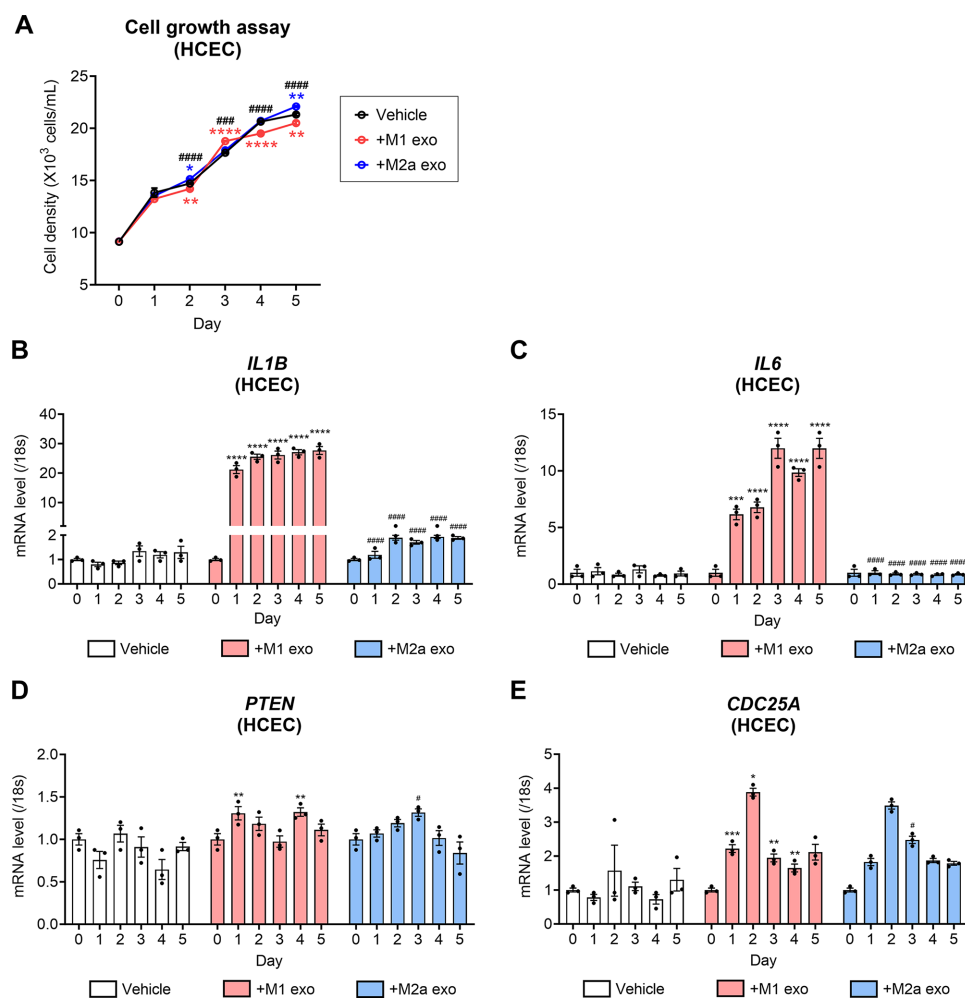


FIGURE 6. Cell growth analysis and gene expression analysis in HCECs treated with M1 and M2a macrophage-derived exosomes under non-inflammatory conditions. **(A)** Growth curves of HCECs treated with M1-exo or M2a-exo compared to naïve HCECs (vehicle) over 5 days. Data are presented as mean \pm SEM from five samples ($n = 5$). **** $P < 0.0001$, ** $P < 0.01$, * $P < 0.05$, **** $P < 0.0001$, *** $P < 0.001$. Red and blue asterisks (*) indicate comparisons of the vehicle group with the M1-exo and M2a-exo groups, respectively. Hash symbols (#) indicate comparisons between the M1-exo and the M2a-exo groups. **(B–E)** qRT-PCR analysis of *IL1B*, *IL6*, *PTEN*, and *CDC25A* mRNA expression in HCECs treated with M1-exo or M2a-exo over 5 days. Data are presented as mean \pm SEM from three samples ($n = 3$). **** $P < 0.0001$, *** $P < 0.001$, ** $P < 0.01$, * $P < 0.05$, **** $P < 0.0001$, # $P < 0.05$; ns, not significant.

late HCEC proliferation via cell cycle activation. Future studies are needed to determine whether increasing exosome dosage or modifying EGF preconditioning strategies could further enhance regenerative outcomes.

One limitation of this study is that it was conducted primarily in vitro and thus did not fully capture the complex interactions present in the corneal microenvironment. The successful in vivo translation of exosome-based therapies will require further investigation into delivery strategies, ocular biodistribution, dosing regimens, and potential immune responses. Addressing these challenges will be essential for advancing the clinical application of macrophage-derived exosomes in corneal endothelial inflammation and regeneration. Especially, in vivo studies using animal models of corneal inflammation and injury will be critical to validate the therapeutic potential of EGF-conditioned M2a macrophage-derived exosomes. Subsequent long-term studies on safety and efficacy will also be necessary before considering clinical translation. Nonetheless, our results highlight the potential of modu-

lating macrophage phenotype to enhance the therapeutic properties of their secreted exosomes. This concept may be further extended to other growth factors or small molecules capable of regulating macrophage function, paving the way for the development of “designer” exosomes with tailored therapeutic effects.

Another important limitation is the lack of direct investigation into the downstream signaling pathways influenced by M2a- or EGF-M2a-derived exosomes. Although our findings clearly demonstrate their anti-inflammatory effects, the specific intracellular mechanisms remain unclear. Future studies employing omics-based proteomic profiling may help identify critical mediators—such as TGF- β 1, tumor necrosis factor-stimulated gene-6 (TSG-6), or IL-10-related cargo—that have been implicated in the immunomodulatory functions of macrophage-derived exosomes.^{42,43} Additionally, pathway-specific inhibition studies targeting signaling cascades such as nuclear factor kappa-light-chain-enhancer of activated B cells (NF- κ B) or mitogen-activated protein kinase (MAPK) may provide further insight into the molecu-

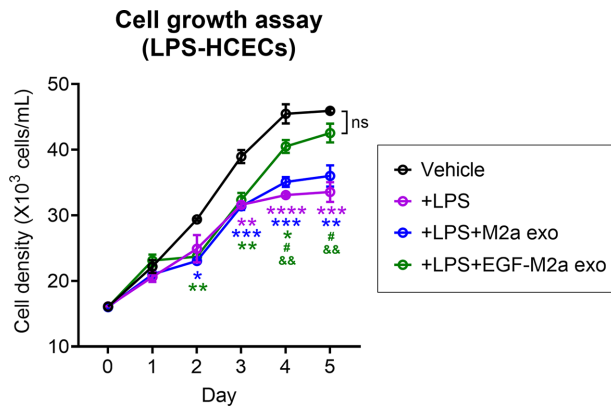


FIGURE 7. Cell growth analysis of LPS-induced inflammatory HCECs treated with M2a-exo or EGF-M2a-exo. Growth curves of LPS-HCECs treated with M2a-exo or EGF-M2a-exo compared to naïve HCECs (vehicle) and untreated LPS-HCECs, over 5 days. Data are presented as mean \pm SEM from three samples ($n = 3$). **** $P < 0.0001$, *** $P < 0.001$, ** $P < 0.01$, * $P < 0.05$, # $P < 0.05$, & $P < 0.01$; ns, not significant. Purple, blue, and green asterisks (*) indicate comparisons of the vehicle group with the LPS, LPS+M2a-exo, and LPS+EGF-M2a-exo groups, respectively. Green hash symbols (#) indicate comparisons between the LPS+EGF-M2a-exo group and the LPS+M2a-exo group. Green ampersand symbols (&) indicate comparisons between the LPS+EGF-M2a-exo group and the LPS group.

lar mechanisms by which these exosomes exert their effects in HCECs.

Exosome-based therapies are being actively explored in various fields, including the use of mesenchymal stem cell-derived exosomes for treating liver injury, myocardial infarction, and spinal cord injury, due to their potent anti-inflammatory and regenerative properties.^{44–46} These previous studies support the broader translational relevance of our findings for ocular surface disease.

In conclusion, this study highlights the potential of M2a macrophage-derived exosomes as a novel therapeutic strategy for managing corneal endothelial inflammation and injury. We demonstrated that M2a macrophage-derived exosomes effectively suppress inflammatory responses in a simple LPS-induced model using HCECs, although their efficacy was limited under the more complex dual inflammation-and-wound condition. Notably, EGF preconditioning enhanced the anti-inflammatory and pro-regenerative capacities of M2a macrophage-derived exosomes, restoring their efficacy even in severe inflammatory settings. Future research should focus on optimizing the large-scale production of therapeutic M2a macrophage-derived exosomes and refining approaches to enhance M2a macrophage differentiation and function in vivo, particularly within the ocular surface environment.

Acknowledgments

Supported by grants from the National Research Foundation of Korea, funded by the Korean government (RS-2023-00209498, RS-2023-00219421); by a grant from the Korea Health Technology R&D Project through the Korea Health Industry Development Institute, funded by the Ministry of Health & Welfare, Republic of Korea (RS-2024-00438366); and by a research grant from the Korea Medical Institute.

Disclaimer: **S.H. Lee**, None; **A. Koh**, None; **S.J. Lee**, None; **H. Lee**, None; **K.W. Kim**, None

References

- Bourne WM. Biology of the corneal endothelium in health and disease. *Eye (Lond)*. 2003;17:912–918.
- Joyce NC. Proliferative capacity of the corneal endothelium. *Prog Retin Eye Res*. 2003;22:359–389.
- Bonanno JA. Molecular mechanisms underlying the corneal endothelial pump. *Exp Eye Res*. 2012;95:2–7.
- Sagoo P, Chan G, Larkin DF, George AJ. Inflammatory cytokines induce apoptosis of corneal endothelium through nitric oxide. *Invest Ophthalmol Vis Sci*. 2004;45:3964–3973.
- Shivanna M, Rajashekhar G, Srinivas SP. Barrier dysfunction of the corneal endothelium in response to TNF- α : role of p38 MAP kinase. *Invest Ophthalmol Vis Sci*. 2010;51:1575–1582.
- Gain P, Jullienne R, He Z, et al. Global survey of corneal transplantation and eye banking. *JAMA Ophthalmol*. 2016;134:167–173.
- Chinnery HR, McMenamin PG, Dando SJ. Macrophage physiology in the eye. *Pflügers Arch*. 2017;469:501–515.
- Knickelbein JE, Watkins SC, McMenamin PG, Hendricks RL. Stratification of antigen-presenting cells within the normal cornea. *Ophthalmol Eye Dis*. 2009;1:45–54.
- Seyed-Razavi Y, Chinnery HR, McMenamin PG. A novel association between resident tissue macrophages and nerves in the peripheral stroma of the murine cornea. *Invest Ophthalmol Vis Sci*. 2014;55:1313–1320.
- Hamrah P, Liu Y, Zhang Q, Dana MR. The corneal stroma is endowed with a significant number of resident dendritic cells. *Invest Ophthalmol Vis Sci*. 2003;44:581–589.
- Mantovani A, Sica A, Sozzani S, Allavena P, Vecchi A, Locati M. The chemokine system in diverse forms of macrophage activation and polarization. *Trends Immunol*. 2004;25:677–686.
- Murray PJ, Wynn TA. Protective and pathogenic functions of macrophage subsets. *Nat Rev Immunol*. 2011;11:723–737.
- Liu J, Xue Y, Dong D, et al. CCR2(–) and CCR2(+) corneal macrophages exhibit distinct characteristics and balance inflammatory responses after epithelial abrasion. *Mucosal Immunol*. 2017;10:1145–1159.
- Martinez FO, Gordon S. The M1 and M2 paradigm of macrophage activation: time for reassessment. *F1000Prime Rep*. 2014;6:13.
- Rószter T. Understanding the mysterious M2 macrophage through activation markers and effector mechanisms. *Mediators Inflamm*. 2015;2015:816460.
- Ferrante CJ, Leibovich SJ. Regulation of macrophage polarization and wound healing. *Adv Wound Care (New Rochelle)*. 2012;1:10–16.
- Larkin DF, Calder VL, Lightman SL. Identification and characterization of cells infiltrating the graft and aqueous humour in rat corneal allograft rejection. *Clin Exp Immunol*. 1997;107:381–391.
- Becker MD, Planck SR, Crespo S, et al. Immunohistology of antigen-presenting cells in vivo: a novel method for serial observation of fluorescently labeled cells. *Invest Ophthalmol Vis Sci*. 2003;44:2004–2009.
- Zheng M, Deshpande S, Lee S, Ferrara N, Rouse BT. Contribution of vascular endothelial growth factor in the neovascularization process during the pathogenesis of herpetic stromal keratitis. *J Virol*. 2001;75:9828–9835.
- Kalluri R, LeBleu VS. The biology, function, and biomedical applications of exosomes. *Science*. 2020;367:eaau6977.
- Lee SJ, Lee SH, Koh A, Kim KW. EGF-conditioned M1 macrophages convey reduced inflammation into corneal endothelial cells through exosomes. *Heliyon*. 2024;10:e26800.

22. Zhang Q, Fu L, Liang Y, et al. Exosomes originating from MSCs stimulated with TGF- β and IFN- γ promote Treg differentiation. *J Cell Physiol.* 2018;233:6832–6840.
23. Zhao H, Shang Q, Pan Z, et al. Exosomes from adipose-derived stem cells attenuate adipose inflammation and obesity through polarizing M2 macrophages and beiging in white adipose tissue. *Diabetes.* 2018;67:235–247.
24. Kim KW, Park SH, Lee SJ, Kim JC. Ribonuclease 5 facilitates corneal endothelial wound healing via activation of PI3-kinase/Akt pathway. *Sci Rep.* 2016;6:31162.
25. Lee SJ, Koh A, Lee SH, Kim KW. Distinct activation of M1 and M2 macrophages in the primary pterygium lymphangiogenesis. *Exp Eye Res.* 2024;248:110108.
26. Lee SJ, Koh A, Lee SH, Kim KW. Efficacy of epidermal growth factor in suppressing inflammation and proliferation in pterygial fibroblasts through interactions with microenvironmental M1 macrophages. *Sci Rep.* 2024;14:22601.
27. Genin M, Clement F, Fattaccoli A, Raes M, Michiels C. M1 and M2 macrophages derived from THP-1 cells differentially modulate the response of cancer cells to etoposide. *BMC Cancer.* 2015;15:577.
28. Ankley LM, Conner KN, Vielma TE, Godfrey JJ, Thapa M, Olive AJ. GSK3 α/β restrain IFN- γ -inducible costimulatory molecule expression in alveolar macrophages, limiting CD4 $^{+}$ T cell activation. *Immunohorizons.* 2024;8:147–162.
29. Ibanez-Esparza MO, González-Salinas R, Concha-Del-Río LE, Navarro-López P. Findings in corneal endothelium by confocal and specular microscopy in patients with Fuchs uveitis syndrome undergoing phacoemulsification. *Ocul Immunol Inflamm.* 2024;33:432–438.
30. Yoshida M, Yokoyama Y, Kokubun T, et al. Long-term surgical outcomes and possible postoperative complication with severe corneal endothelial cell loss after trabeculectomy for cytomegalovirus-associated anterior uveitis with secondary glaucoma. *Ocul Immunol Inflamm.* 2024;32:690–698.
31. Joyce NC. Proliferative capacity of corneal endothelial cells. *Exp Eye Res.* 2012;95:16–23.
32. Peh GS, Toh KP, Wu FY, Tan DT, Mehta JS. Cultivation of human corneal endothelial cells isolated from paired donor corneas. *PLoS One.* 2011;6:e28310.
33. Yin J, Xu K, Zhang J, Kumar A, Yu FS. Wound-induced ATP release and EGF receptor activation in epithelial cells. *J Cell Sci.* 2007;120:815–825.
34. Yamazoe K, Yamaguchi T, Hotta K, et al. Outcomes of cataract surgery in eyes with a low corneal endothelial cell density. *J Cataract Refract Surg.* 2011;37:2130–2136.
35. Downs KP, Nguyen H, Dorfleitner A, Stehlik C. An overview of the non-canonical inflammasome. *Mol Aspects Med.* 2020;76:100924.
36. Jiang L, Zhang S, Hu H, et al. Exosomes derived from human umbilical cord mesenchymal stem cells alleviate acute liver failure by reducing the activity of the NLRP3 inflammasome in macrophages. *Biochem Biophys Res Commun.* 2019;508:735–741.
37. Pavilack MA, Elner VM, Elner SG, Todd RF, 3rd, Huber AR. Differential expression of human corneal and perilimbal ICAM-1 by inflammatory cytokines. *Invest Ophthalmol Vis Sci.* 1992;33:564–573.
38. Lu N, Wang L, Cao H, et al. Activation of the epidermal growth factor receptor in macrophages regulates cytokine production and experimental colitis. *J Immunol.* 2014;192:1013–1023.
39. Eming SA, Wynn TA, Martin P. Inflammation and metabolism in tissue repair and regeneration. *Science.* 2017;356:1026–1030.
40. Karin M, Clevers H. Reparative inflammation takes charge of tissue regeneration. *Nature.* 2016;529:307–315.
41. Pastore S, Mascia F, Mariani V, Girolomoni G. The epidermal growth factor receptor system in skin repair and inflammation. *J Invest Dermatol.* 2008;128:1365–1374.
42. Hade MD, Suire CN, Suo Z. Mesenchymal stem cell-derived exosomes: applications in regenerative medicine. *Cells.* 2021;10:1959.
43. Ilg MM, Bustin SA, Ralph DJ, Cellek S. TGF- β 1 induces formation of TSG-6-enriched extracellular vesicles in fibroblasts which can prevent myofibroblast transformation by modulating Erk1/2 phosphorylation. *Sci Rep.* 2024;14:12389.
44. Lai RC, Arslan F, Lee MM, et al. Exosome secreted by MSC reduces myocardial ischemia/reperfusion injury. *Stem Cell Res.* 2010;4:214–222.
45. Lou G, Chen Z, Zheng M, Liu Y. Mesenchymal stem cell-derived exosomes as a new therapeutic strategy for liver diseases. *Exp Mol Med.* 2017;49:e346.
46. Xin H, Li Y, Cui Y, Yang JJ, Zhang ZG, Chopp M. Systemic administration of exosomes released from mesenchymal stromal cells promote functional recovery and neurovascular plasticity after stroke in rats. *J Cereb Blood Flow Metab.* 2013;33:1711–1715.